

Non Linear Behavior of Steel Fibrous Prestressed Frames under Cyclic Loads

Dr. Bayar J. Al-Sulayfani

Assistant Professor

College of Engineering/ Civil Department
University of Mosul-Iraq

Hatim T. Al-Tae

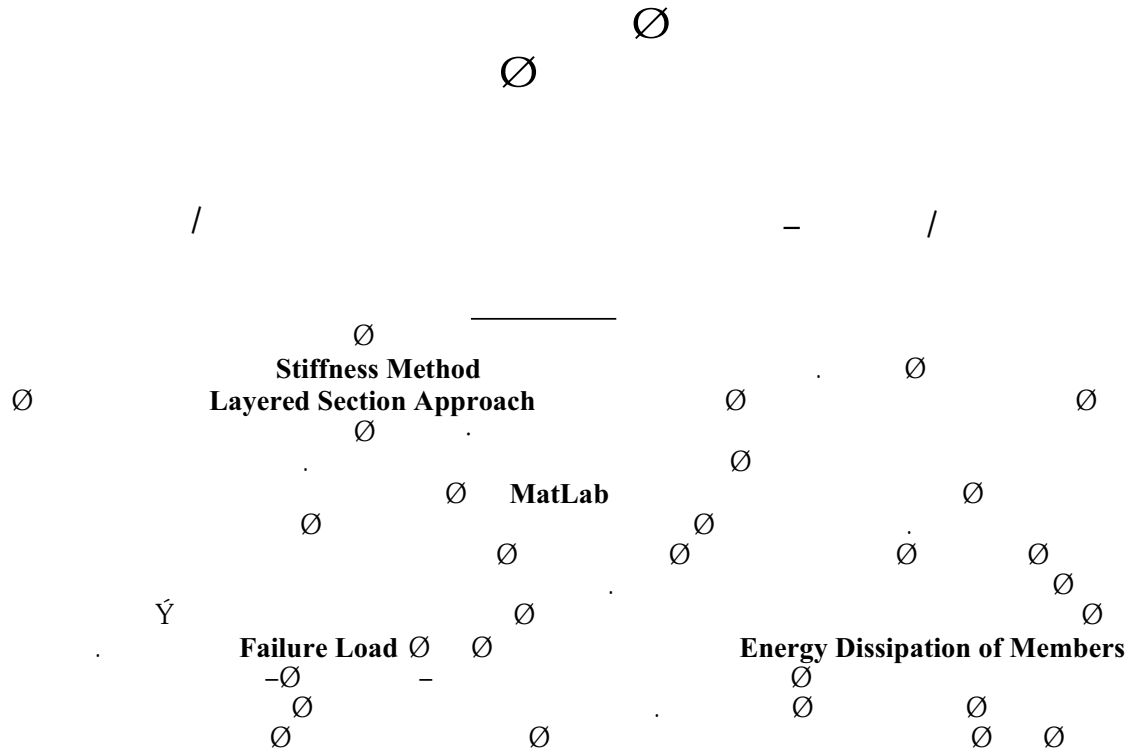
Badush Dam Project Iraq
Ministry of Water Resources

Abstract

This paper presents a numerical model which is capable of predicting the behavior of fibrous prestressed concrete beams and frames subjected to cyclic loads. The stiffness method with the effective secant stiffness is used here in analyzing plane structures, while the analysis of member cross sections that are subjected to cyclic loads is carried out in combination with the layered section approach. Material nonlinearity has been taken in to consideration through the analysis of these sections. This method deals only with axial forces and bending moments neglecting the effect of shear forces. The study presents a program written with **MATLAB** language that analyzes structures by the STIFFNESS method and divides the cross sections into small layers in order to utilize the nonlinearity of the stress distribution along the section depth. The results at each section are moments, curvatures, displacements, forces, stresses and strains under each load cycle. A cyclic model for fibrous concrete subjected to uniaxial compression or tension has been proposed. Also the cyclic model of Menegotto and Pinto for conventional and prestressing steel has been adopted. Full bond between steel and concrete is assumed.

The study shows that the prestressing force in concrete members has reduced the ductility or capacity of energy dissipation, while a noticeable increase in the member failure load is recorded. Moreover, the existence of steel fibers in concrete enhances its stiffness, delays the cracks and then narrows their openings in tension zone and decreases their negative effect. The layered section presents more reliable stress distribution on the cross section of the concrete members.

Keywords: Concrete, Cyclic Load, Frames, Prestress , Steel fiber.



Received 7th Nov. 2004

Accepted 22nd Jun 2005

Introduction

The behavior of steel fiber reinforced concrete members subjected to cyclic loads is extremely complex. It is necessary to make use of numerical solutions in solving non linear governing equations established by the material nonlinearities and the effect of large displacements in concrete structures since finding analytic solutions seems to be more complicated. The finite element method has been used by several researchers [1] [2] to analyze reinforced and prestressed concrete members considering material nonlinearity. While the stiffness method with tangent and secant stiffnesses was used by others [3-5] to analyze the reinforced concrete frames under monotonic loading. This paper presents a more practical MATLAB computer program developed for an elastic–plastic analysis of plane frames. It takes into account the materials nonlinearity of steel fibrous concrete, reinforcing steel and prestressed tendons embedded in the sections of concrete members. In order to get a proper prediction for the behavior of prestressed fibrous concrete structure under cyclic loading, constitutive relationships for steel fiber concrete, conventional steel and prestressing steel wires are required. Fibrous Concrete in Cyclic Compression The cyclic behavior model of the steel fiber concrete under uniaxial compression shown in Fig. (1) is adopted, where the monotonic stress–strain curve [6] represents the envelope for the cyclic behavior paths.

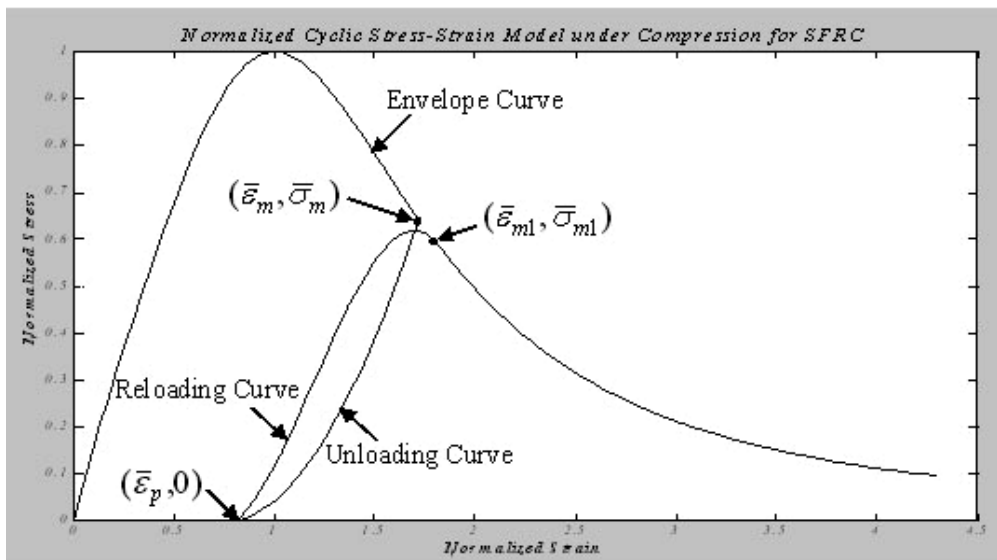


Fig. (1): Cyclic Model of steel fiber concrete under compression

The following equation recommended in Ref. [6] was used for the envelope curve:

$$\bar{\sigma} = \frac{A \cdot \bar{\epsilon}}{\bar{\epsilon}^3 + B \cdot \bar{\epsilon}^2 + C \cdot \bar{\epsilon} + D} \dots\dots\dots (1)$$

Where: $\bar{\sigma} = \frac{\sigma}{f_{c_f}}$ is the normalized peak stress of steel fiber concrete

$\bar{\varepsilon} = \frac{\varepsilon}{\varepsilon_{of}}$ is the normalized strain at peak stress of SFC

\bar{f}_{c_f} are coefficients depend on the percent of steel fiber content A, B, C, D ($V_f\%$), maximum aggregate size and the maximum cylinder compressive f_{c_f} strength

The unloading path presented in this paper (Fig. (1)) is that proposed by Ref. [7]:

$$(2) \dots\dots\dots \bar{\sigma}_u = C_u \bar{\sigma}_m \left| \frac{\bar{\varepsilon}_u - \bar{\varepsilon}_p}{\bar{\varepsilon}_m - \bar{\varepsilon}_p} \right|^{n_u}$$

where: $\bar{\sigma}_u = \frac{\sigma_u}{f_c}$ is the normalized stress on the reloading curve.

$\bar{\varepsilon}_u = \frac{\varepsilon_u}{\varepsilon_o}$ is the normalized strain on the reloading curve.

$C_u \approx 0.95 - 1.0$ is unloading coefficient

$\bar{\sigma}_m = \frac{\sigma_m}{f_c}$ is the normalized stress at the unloading point.

$\bar{\varepsilon}_m = \frac{\varepsilon_m}{\varepsilon_o}$ is the normalized strain at the unloading point.

$n_u = 1 + \sqrt{\bar{\varepsilon}_p} \geq 1$ is a coefficient (function of the plastic strain).

The amount of plastic strain for each full unloading is evaluated as follow [8]:

$$(3) \dots\dots\dots \bar{\varepsilon}_p = \begin{cases} 0.055 \bar{\varepsilon}_m + 0.127 (\bar{\varepsilon}_m)^{3.1} & \text{for } \bar{\varepsilon}_m \leq 2.2 \\ 1.584 + 0.72 (\bar{\varepsilon}_m - 2.2) & \text{for } \bar{\varepsilon}_m > 2.2 \end{cases}$$

where: $\bar{\varepsilon}_p = \frac{\varepsilon_p}{\varepsilon_o}$ is the normalized plastic strain.

$\bar{\varepsilon}_m = \frac{\varepsilon_m}{\varepsilon_o}$ is the normalized unloading strain on the envelope curve.

The reloading strain value on the envelope curve for each full reloading was expressed by the formula [9]:

$$\bar{\varepsilon}_{m1} = \bar{\varepsilon}_m + k_r$$

Where: $k_r = \begin{cases} 0.0 & \text{for } \bar{\varepsilon}_{m1} \leq 1 \\ 0.1 & \text{for } \bar{\varepsilon}_{m1} > 1 \end{cases}$ (4)

For each unloading, the reloading curve has the following equation [8]:

$$\bar{\sigma}_r = A_r \bar{\varepsilon}_r^3 + B_r \bar{\varepsilon}_r^2 + C_r \bar{\varepsilon}_r + D_r \quad \dots\dots\dots(5)$$

Where: $\bar{\sigma}_r$: is the normalized stress on the reloading curve.

$\bar{\varepsilon}_r$: is the normalized strain on the reloading curve.

A_r, B_r, C_r, D_r is the reloading coefficients.

, the boundary conditions are: A_r, B_r, C_r, D_r To solve for the coefficients

1. The polynomial passes though the normalized plastic strain point $(\bar{\varepsilon}_p, 0)$.
2. The polynomial passes though the normalized reloading strain point $(\bar{\varepsilon}_{m1}, \bar{\sigma}_{m1})$.
3. The slope of the polynomial at the normalized reloading strain point exactly coincides with the slope of the monotonic curve at the same point; i.e. $(E_{r(\bar{\varepsilon}_{m1}, \bar{\sigma}_{m1})} = E_{c(\bar{\varepsilon}_{m1}, \bar{\sigma}_{m1})})$.
4. The following expression would be satisfied:

$$\frac{E_{r(\bar{\varepsilon}_p, 0)}}{E_{c_{0.45}}} = \frac{1}{(0.95 + 2.78\bar{\varepsilon}_p)} \quad \dots\dots\dots(6)$$

Where: $E_{r(\bar{\varepsilon}_p, 0)}$ = the slope of the polynomial at the plastic strain

$E_{c_{0.45}}$ = the slope of the monotonic curve at $0.45\bar{f}_{cf}$

\bar{f}_{cf} = the ultimate compressive strength of fibrous concrete

Fibrous Concrete in Cyclic Tension

A, B, C, D To model the behavior of concrete under cyclic tension, equation (1) can be used with different coefficients :

$$\bar{\sigma}_t = \frac{A \cdot \bar{\varepsilon}_t}{\bar{\varepsilon}_t^3 + B \cdot \bar{\varepsilon}_t^2 + C \cdot \bar{\varepsilon}_t + D} \quad \dots\dots\dots(7)$$

where: $\bar{\sigma}_t = \frac{\sigma_t}{f_t}$ is the normalized maximum tensile strength in MPa .

Al-Sulafani : Non linear behavior of steel fibrous prestressed frames under C.L

$\bar{\varepsilon}_t = \frac{\varepsilon_t}{\varepsilon_{t_0}}$ is the normalized strain at maximum tensile strength

$\bar{f}_t = 0.5\sqrt{\bar{f}_c}$ is the maximum tensile strength for plain concrete in MPa [10].

$$A = 0.5337, \quad B = -1.9394, \quad C = 1.4127, \quad D = 0.0605$$

$$\text{Soroushian and } \varepsilon_{t_0} = 0.000198 + 0.000075\bar{f}_t \quad \dots\dots (8) \quad \text{Ref. [8]}$$

Lee [11] proposed the following equations to evaluate the tensile strength and the corresponding strain for SFR based on plain concrete:

$$f_{t_f} = \bar{f}_t \cdot (1 + 0.016N_f^{\frac{1}{3}} + 0.05\pi \cdot d_f \cdot l_f \cdot N_f) \quad (9)$$

$$\varepsilon_{t_{of}} = \varepsilon_{t_0} (1 + 0.35N_f \cdot d_f \cdot l_f) \quad (10)$$

Where: $N_f = \frac{1.64V_f}{\pi \cdot d_f^2}$ A linear path was adopted for the cyclic behavior of concrete

under tension with modulus of elasticity equals to the nominal modulus of elasticity in compression. This is valid up to the cracking strength.

Fig. (2) and Fig. (3) show the cyclic tension model of SFRC used in the current study.

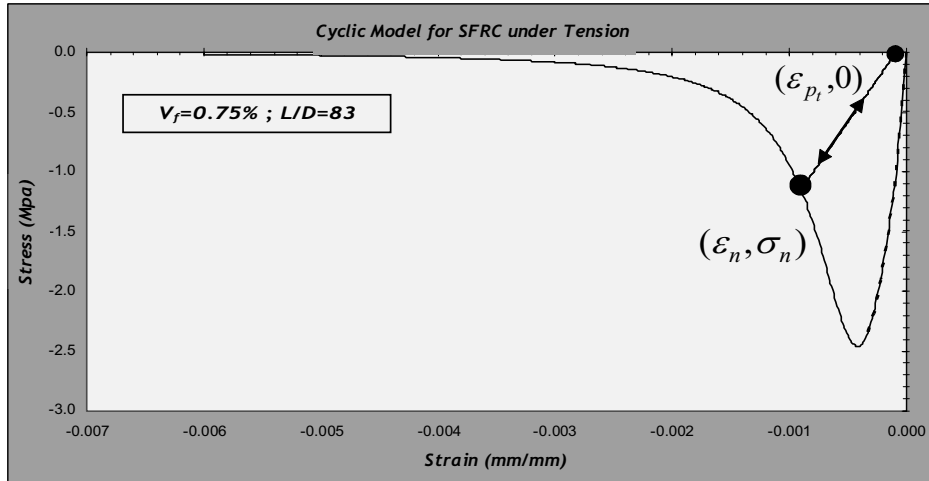


Fig. (2): Cyclic model of steel fiber concrete under uniaxial tension

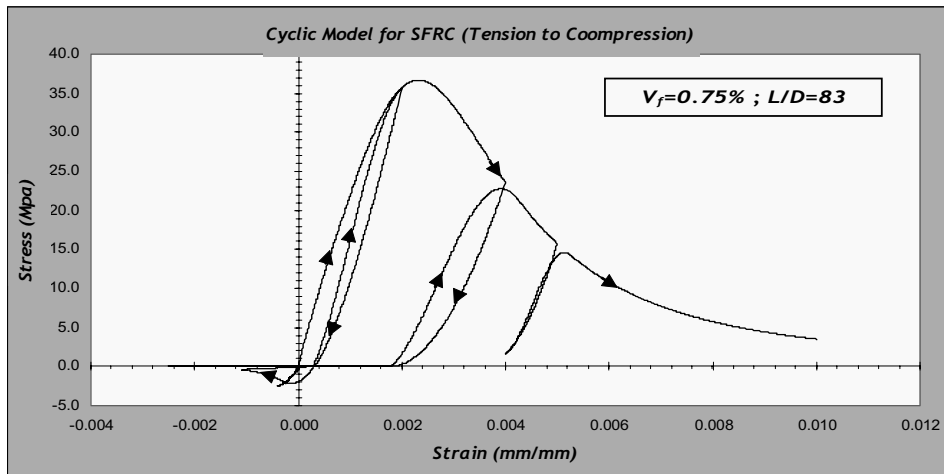


Fig. (3): Cyclic model of SFR under uniaxial tension–compression

Steel Reinforcement in Cyclic Stresses

For uniaxial stress–strain relationship of reinforcing and prestressing steel, the Menegotto and Pinto [12] model is adopted as in Fig. (4). The stress–strain curves of all cycles lie within the two parallel lines of slope b defined () respectively. All these ϵ^2_o, σ^2_o), $(\epsilon^1_o, \sigma^1_o$ by the monotonic curve and passing through the yield points (curves have the same initial slope equal to the slope E_0 of the monotonic curve.

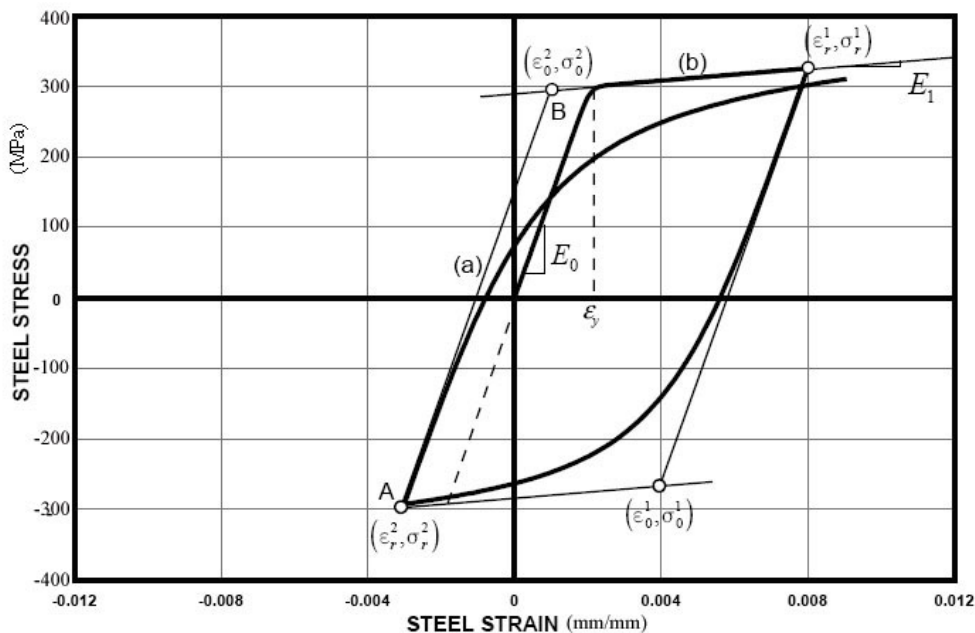


Fig. (4): Menegotto and Pinto Cyclic model for reinforcing steel

For each half cycle of the stress–strain curve the following equation is proposed in a normalized form:

$$\sigma^* = b \cdot \varepsilon^* + \frac{(1-b) \cdot \varepsilon^*}{(1 + \varepsilon^{*R})^{\frac{1}{R_r}}} \quad \dots\dots\dots (11)$$

Where: b is the strain hardening ratio (slope E_1 /slope E_0).

For the curves after the first load inversion:

$$\varepsilon^* = \frac{\varepsilon - \varepsilon_r}{\varepsilon_o - \varepsilon_r}, \quad \sigma^* = \frac{\sigma - \sigma_r}{\sigma_o - \sigma_r} \quad \dots\dots\dots (12)$$

is found by solving the equations of the two $(\varepsilon_o, \sigma_o)$ is the start of the i^{th} inversion, $(\varepsilon_r, \sigma_r)$ where intersecting lines as in Fig. (5).

The exponent R varies after every inversion and is calculated as follows:

$$R = R_o - \frac{a_1 \cdot \xi}{a_2 + \xi} \quad \dots\dots\dots (13)$$

Where R_o, a_1, a_2 , are parameters chosen for the best correlation between experimental and predicted stress–strain curves. ξ is the plastic deformation undergone in each half cycle as shown in Fig. (5).

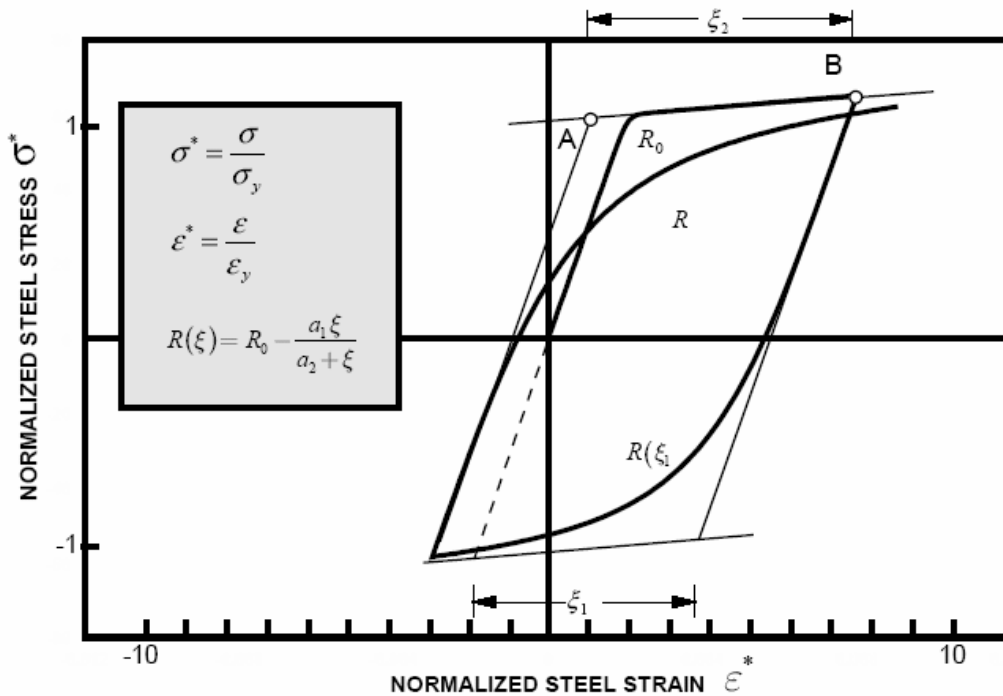
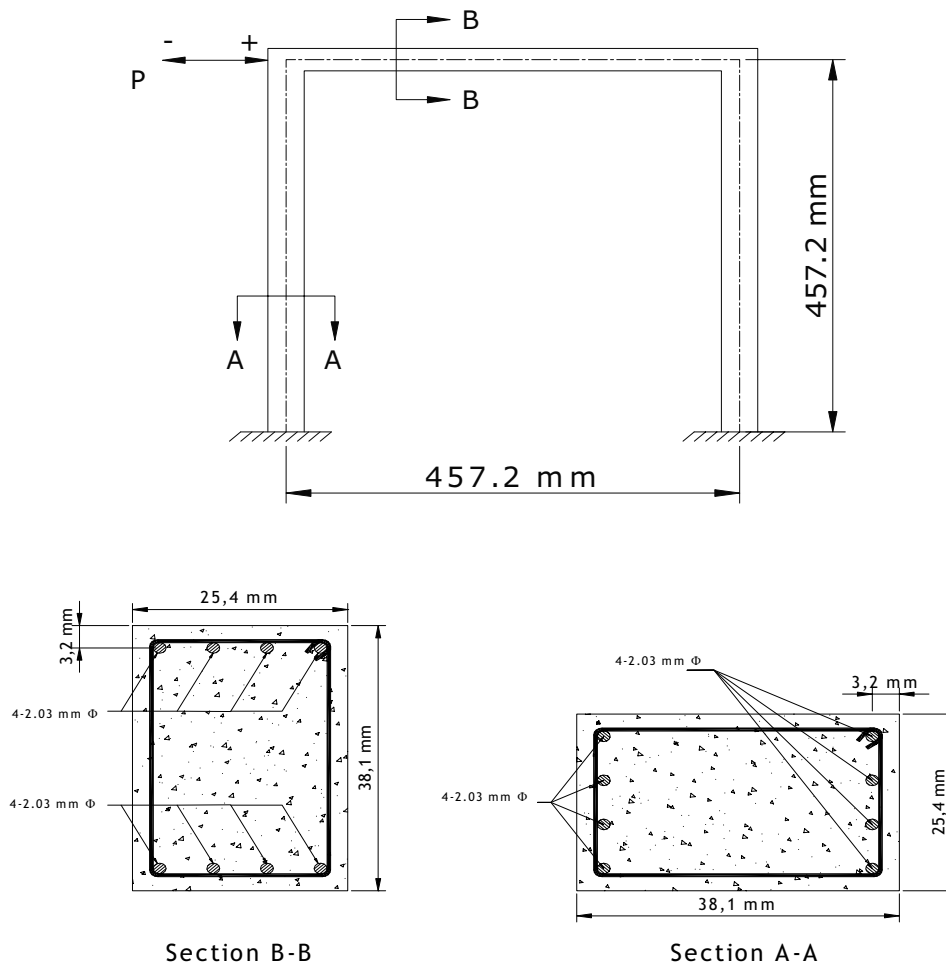


Fig. (5): Definition of factor R in Menegotto and Pinto Cyclic Steel model



Section B-B

Section A-A

Fig. (6): The frame model tested by White and Sabnis [13]

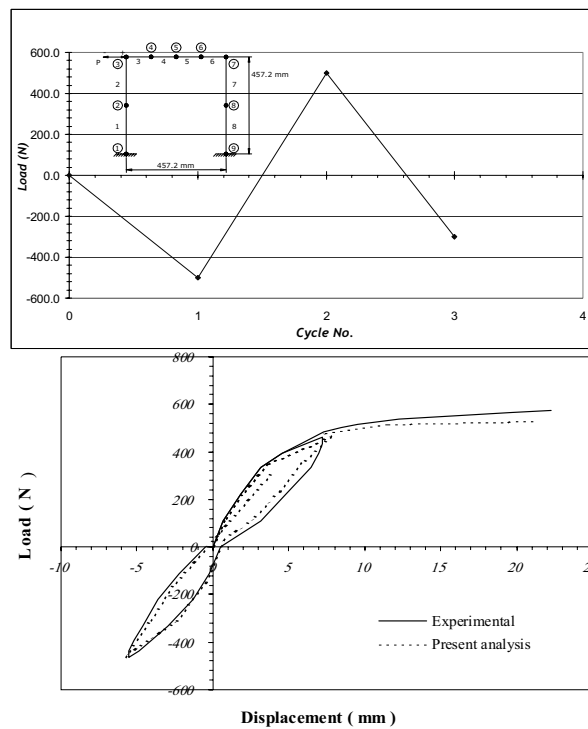


FIG (7): Load –Deflection curve at node 3 (horizontal displacement)

Nonlinear Sectional Analysis

To account for the heterogeneous section, it is divided into imaginary concrete layers, reinforcing and prestressing bar elements, each is analyzed separately. The plane section and the perfect bonding hypothesis permits the calculation of the longitudinal strain in each element of concrete, reinforcing steel and prestressing are \bar{M} and bending moment \bar{P} tendon as a function of the top and bottom fiber strain. The internal axial force calculated as follows:

$$\bar{P} = \sum_{i=1}^m f_{c_i} \cdot A_{c_i} + \sum_{i=1}^n f_{s_i} \cdot A_{s_i} + \sum_{i=1}^{n_p} f_{p_i} \cdot A_{p_i} \quad (14)$$

$$\bar{M} = \sum_{i=1}^m f_{c_i} \cdot A_{c_i} \cdot \left(\frac{H}{2} - Y_{c_i} \right) + \sum_{i=1}^n f_{s_i} \cdot A_{s_i} \cdot \left(\frac{H}{2} - Y_{s_i} \right) \quad \dots\dots\dots (15)$$

To compute the internal and external actions (axial force and bending moment), the top and bottom strain will be corrected iteratively until the two internal actions nearly equal to the external actions within the tolerable limit

Nonlinear Frame Analysis

The linear stiffness method for a frame divided into sub members with uncracked section will be used in the and shear force elastic range initially. As a result, three actions at each end (axial force F_A , bending moment M_B can be ϕ of each section and the curvature ε_{cl} will be obtained); from which the strain at the center line F_S obtained.

at each section is calculated as follows: I_e and effective moment of inertia A_e The effective area

$$A_e = \frac{F_A}{(\varepsilon_{cl} \times E_c)} \quad (16)$$

$$I_e = \frac{M_B}{(\phi \times E_c)} \quad (17)$$

Where E_c is the modulus of elasticity for concrete. To evaluate the equivalent effective area A_x and effective moment of inertia I_z for each member, the interpolated values of the two ends were recommended as follows:

$$I_z = I_o \left[1 - \left[\frac{(1 - \frac{I_{e1}}{I_o})^5 + (1 - \frac{I_{e2}}{I_o})^5}{2} \right]^{\frac{1}{5}} \right] \quad (18)$$

$$A_x = A_o \left[1 - \left[\frac{(1 - \frac{A_{e1}}{A_o})^5 + (1 - \frac{A_{e2}}{A_o})^5}{2} \right]^{\frac{1}{5}} \right] \quad (19)$$

The current calculated values for A_x and I_z for each member are used with the previous values used in the () by taking the average of values: I_{z_p} , A_{x_p} stiffness matrices (

$$A_{x_n} = \frac{A_x + A_{x_p}}{2}, \quad I_{z_n} = \frac{I_z + I_{z_p}}{2}. \quad (20)$$

These values will be used to generate a new stiffness matrix for the next iteration. New axial and flexural stiffnesses are calculated. This procedure will continue until the stiffness values converge to certain values, then the correct displacements, curvatures and actions are computed for a specific loading case.

Results and Discussion

To demonstrate and test the validity of the present method, a comparison has been made with results obtained from a tested model [13] shown in Fig. (6) with the theoretical technique of the current study. Fig. (7) shows a good agreement between the experimental and numerical technique.

A hypothetical prestressed frame is loaded cyclically under 4 modes of loading as shown in Fig. (8). The steel fiber used has an aspect ratio ($L/D = 83$), and the prestressing force is (150 kN). The dimensions and details of section reinforcement for the frame members are shown in Table 1 and Fig. (9).

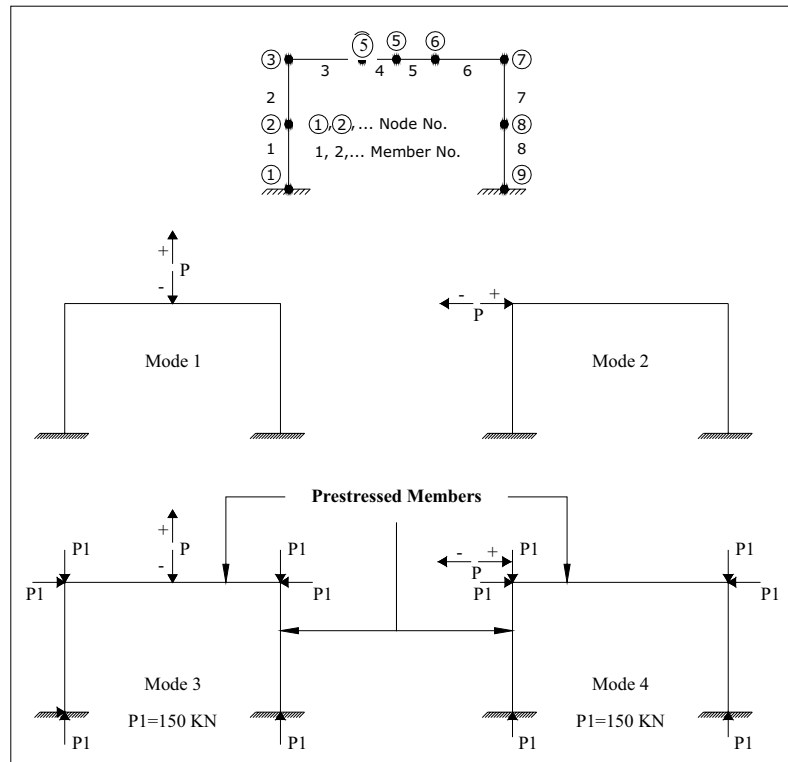


Fig. (8): Loading modes of prestressed hypothetical frame under analysis

Table (1): Dimensions of the frame members

Mode	Member	Width of Section $b(mm)$	Height of section $h(mm)$	Area of reinforcing steel layer in section $A_{s_i}(mm^2)$	Distance from top fiber to the reinforcing steel layer $Y_{s_i}(mm)$	Area of prestressing steel layer in section $A_{p_i}(mm^2)$	Distance from top fiber to the prestressing steel layer $Y_{p_i}(mm)$
• First and second	Beam	300	300	1000	50	-	-
				1000	250	-	-
	Column	300	400	700	50	-	-
				700	200	-	-
• Third and fourth	Beam	300	300	1000	50	150	200
				1000	250	-	-
	Column	300	400	700	50	-	-
				700	200	150	200
				700	350	-	-

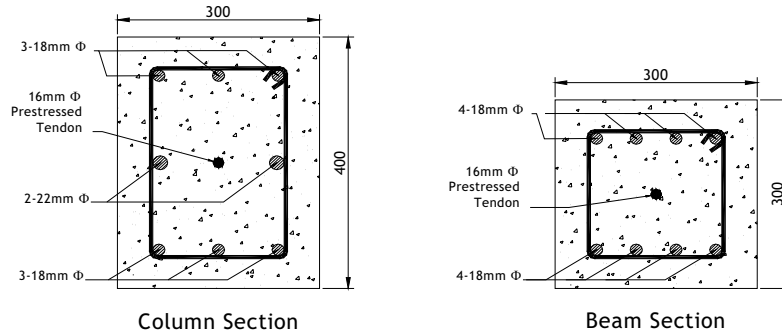


Fig. (9): Details of member cross sections for the hypothetical frame

Figure (10) and Fig. (11) show the load–deflection diagrams for these modes of loading. The general shape of the diagrams looks like an increasing rounded curve as the load increases, with a pinching in shape as the load reverses its direction. It is clear from these figures that the prestressed frame loses its stiffness with the loading history progress where the stiffnesses could be represented by the slope of a line tangent to the load–deflection diagram. The decrease in stiffness is obvious during the loading or unloading increase for a specific cycle or for the repeated cycles at a certain load level. At the pinched part of the curves, the stiffness is reduced due to the opened cracks as the load reverses until the cracks close and the concrete can work in compression.

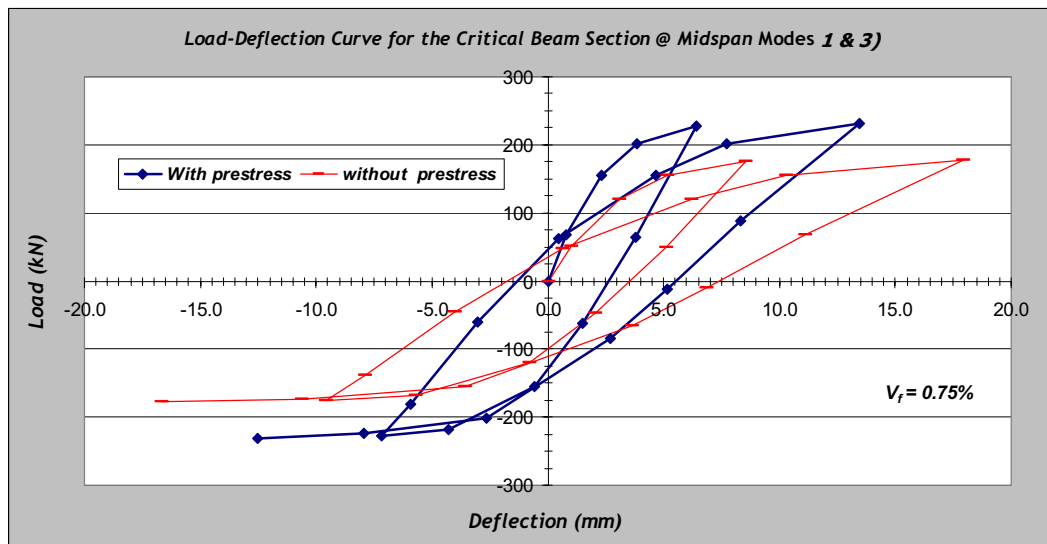


Fig. (10): Load–Deflection Curve for modes 1 and 2

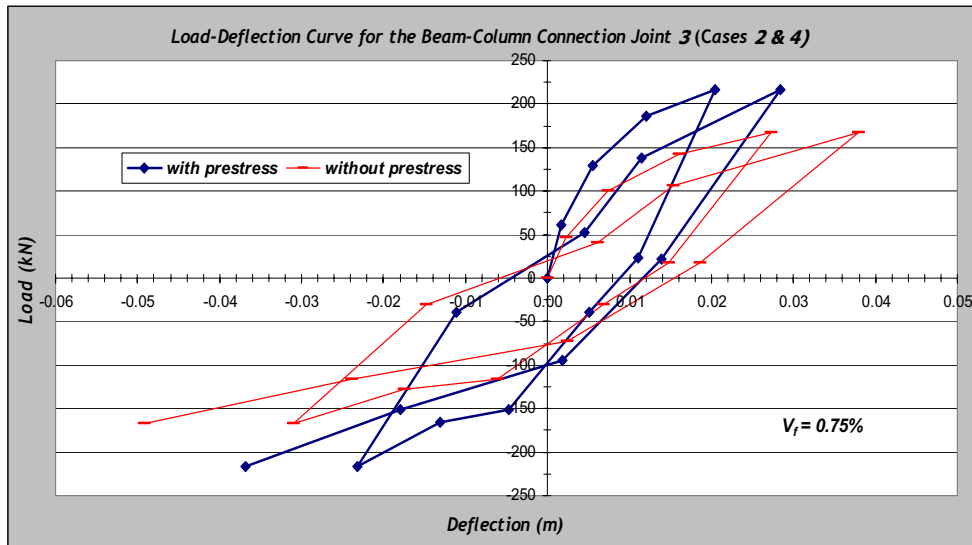


Fig. (11): Load-Deflection Curve for modes 3 and 4

Figure (12) shows the deformed shapes under each loading condition at the center line of the frame in mode 3, with magnified displacements.

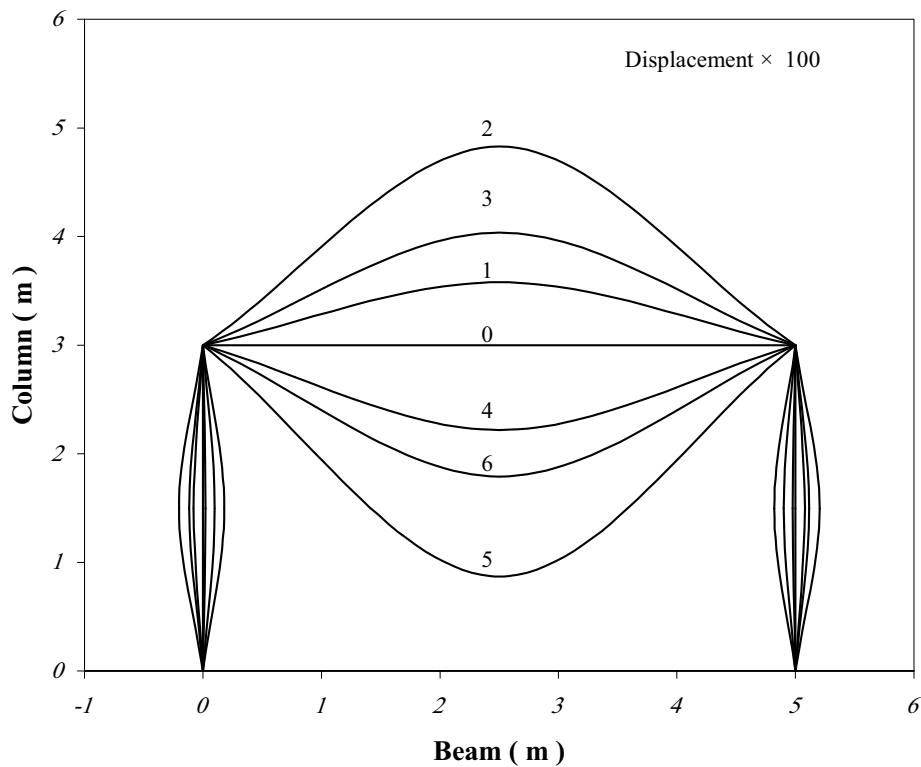


Fig. (12): the deformed shape of a frame cyclically loaded at the center line (Mode 3)

Conclusions

The following main conclusions may be drawn:

1. A true replica of the materials stress–strain characteristics is the basic requirement for simulation of inelastic behavior up to the collapse of ductile structures.
2. This computational technique allows the use of complex material models under cyclic loading and relates them with the structure behavior rather accurately.
3. The major cause of strength and stiffness degradation and the consequent loss of energy dissipation in members is the development of a full depth crack forming a plastic hinged zone.
4. The major cause of strength and stiffness degradation and the consequent loss of energy dissipation in members is the development of a full depth crack forming a plastic hinged zone.
5. The analytic model adopted in this study for the fibrous concrete represented obviously the behavior of steel fiber prestressed concrete frames under cyclic loads. This could be noted through comparing the experimental results of previous studies with those of the present model. Additionally, the model is composed of simple mathematical relationships forming only one nonlinear continuous formula having a high flexibility to deal with and could be developed to fit other possible load conditions.
6. Although the tensile force of the prestressed tendon in concrete members caused a reduction in the ability of these members to dissipate the energy, they increased the values of failure loads for these members.
7. the layer section approach is so efficient in nonlinear analysis of concrete members, since the stress distribution along the sections seems to be rather close to the real state.

References

1. Nilson, A. H., “*Nonlinear analysis of reinforced concrete by finite element method*”, ACI Journal, Sept. 1968, pp. 757-766.
2. Darwin, and Pecknold, A., “*Analysis of Cyclic Loading of Plane R/C Structures*”, Computer and Structures, Vol. 7, 1977, pp. 137-147.
3. Gunnin, B.L., “*Nonlinear Analysis of Planar Frames*”, Ph.D. Dissertation, The University of Texas at Austin, 1970.
4. Sirisreeterux, and Tanabe, “*Nonlinear Analysis of Reinforced Concrete Frames*”, Concrete Engineering and Pavement Division, Vol. 11, 1979, pp. 320-323.
5. Vecchio, F.J., “*Nonlinear Analysis of Reinforced Concrete Frames Subjected to Thermal and Mechanical Loads*”, ACI Structural Journal , Nov.–Dec. 1987, pp. 492-501.
6. Al-Sulayfani, J., “*Analytic Model for Stress-Strain Relationship of Steel Fiber Reinforced Concrete*”, Eng.and Technology Vol. 23,Nov.12,2004
7. Bahn, B. Y. and Hsu, T., “*Stress-Strain Behavior of Concrete Under Cyclic Loading*”, ACI Materials Journal, Vol. 95, No. 2, March-April 1998, pp. 178-193.

8. Al-Sulayfani, J. (1986), "*Contribution a l'etude du comportement des ossatures en beton arme sous sollicitations cycliques par analyse non-lineaire globale*". Docteur de l'Universite de Nantes, Specialite genie Civil.
 9. Otter, E. and Naaman, E., "*Model for Response of Concrete to Random Compressive Loads*", Journal of Structural Engineering ASCE, Vol. 115, No. 11, Nov. 1989, pp. 2794-2809.
 10. Ebrahim, T.M. and N. H. and S. O., "*Biaxial Stress-Strain Relationships for Concrete* ", Magazine of Concrete Research, Vol. 31 , No. 109 , Dec. 1979.
 11. Soroushian and Lee, "*Constitutive Modeling of steel Fiber Reinforced Concrete Under Direct Tension and Compression*", International Conference On Recent Developments in Fiber Reinforced Cements and Concretes, Cardiff, UK, Sep. 1989, pp. 363-377.
 12. Menegotto, M. and Pinto, P. E., "*Method of Analysis for Cyclically Loaded Reinforced Concrete Plane Frames Including Changes in Geometry and Non-Elastic Behavior of Elements under Combined Normal Force and Bending*", Proceedings, IABSE Symposium on Resistance and Ultimate Deformability of Structures Acted on by Well-Defined Repeated Loads, Final Report, Lisbon, 1973, pp. 15-22.
- Sabnis, G. M. and White, R. N., "*Behavior of Reinforced Concrete Frames Under Cyclic Loads Using Small Scale Models*", ACI Materials Journal, Vol. 66, No. 9,